

AN INTERFACE MODEL FOR MIXED-MODE, BUCKLING-DRIVEN DECOHESION OF SUPERFICIAL LAYERS

S. Bennati and P.S. Valvo
Department of Structural Engineering – University of Pisa
Via Diotisalvi, 6 – I 56126 Pisa (PI) – Italy
E-mail: s.bennati@ing.unipi.it, p.valvo@ing.unipi.it

ABSTRACT

The paper presents a mechanical model for describing the phenomenon of mixed-mode buckling-driven decohesion of a thin superficial layer from an underlying substrate loaded in compression. The superficial layer is schematised as a film partly bonded to the substrate by means of an elastic interface, in turn, represented by a continuous distribution of linear elastic springs placed both normally and tangentially to the interface plane. The nonlinear equilibrium problem is solved explicitly, so that the buckling stress is determined together with the complete structural response in the pre- and post-critical phases. In particular, the normal and tangential interfacial stresses are determined, from which the mode-I and mode-II components of the strain energy release rate and the mode-mixity angle are derived. Finally, a mixed-mode crack-growth criterion is applied and different types of possible crack growth predicted by the model are discussed.

Introduction

The detachment of a thin superficial layer from an underlying substrate due to the combined action of local buckling and fracture propagation is a damage mode common to many technological applications and natural situations. For instance, delamination is one of the most insidious attempts on the integrity and the mechanical performances of fibre-reinforced laminated composites [1-2]. An analogous phenomenon is the detachment of a skin from the core of a sandwich plate [3]. Furthermore, the decohesion of a thin film from a substrate is commonly observed in metal elements covered by protective coatings and in microelectronic components, but also in biological structures and so on [4-7]. The essence of the phenomenon is as follows. When the superficial layer is loaded in compression (because of applied loads, thermal mismatch, etc.), the regions where bonding is weak or missing may undergo local buckling. As a consequence, high stresses arise at the contour of the debonded region, thus promoting its further expansion.

As the literature on the subject is very extensive, only a few references can be given here. The first mechanical models, relative to plane-strain problems, were proposed by Kachanov [8] and Chai *et al.* [9]. Thereafter, many theoretical and experimental studies have been carried out and a number of cases analysed. Despite this great research effort over the last twenty-five years, delamination buckling is still a current research topic and many questions, such as crack nucleation, fibre bridging, anisotropy, interface modelling, fatigue growth, mixed-mode growth, and so on, warrant further in-depth investigation. In a buckling-driven decohesion process, the instability and fracture phenomena are closely related and take place simultaneously. However, the prevailing approach in the literature is to analyse these two aspects separately: firstly, the nonlinear equilibrium problem is solved, in the framework of elasticity theory [10] or by structural theories [11]; secondly, a crack-growth criterion is applied. To this aim, local parameters describing the singularity of the stress field at the crack front, such as the stress-intensity factors, k_I , k_{II} , and k_{III} , related to the three modes of crack growth (I or opening, II or sliding, and III or tearing) can be evaluated directly when the post-critical solution is found via elasticity theory [12]. Instead, when a structural model is used, they can be estimated *a posteriori* from the computed solution [13]. A simpler approach is to consider a global parameter, such as the energy release rate, G , for predicting crack growth [14-15]. However, as it was soon recognised for both composites and general layered materials [16-17], experimental values of the fracture toughness are much greater for mode-II or mode-III tests than for mode I. As a consequence, since in general the process of delamination buckling involves a mix of the three modes, any successful attempt to model the phenomenon should take into account a method for evaluating the mode-mixity, *i.e.* the relative amount of the growth modes, and a mixed-mode growth criterion should be adopted [18-19].

A more detailed description of the process of layer separation can be achieved through the theory of interfaces [20-21], which can be included within the framework of a structural model in order to gain information about the stress components acting between the separating layers. The simplest interface that can be imagined is probably a continuous distribution of linear elastic springs [22-23]. The Authors of the present paper have proposed elsewhere [24-25] a model for describing delamination buckling and growth in composite laminated plates loaded in compression, where a delaminated plate is modelled as the union of two sublaminates of finite thickness, partly bonded together by an elastic interface. The sublaminates are modelled according to von Kármán's plate theory. The interface is schematised as a continuous distribution of linear elastic

springs acting in both the normal and tangential directions with respect to the interface plane. In the simpler case of a through-the-width delamination, explicit expressions were determined for the solution of the equilibrium problem in both the pre- and post-critical phases. Moreover, the normal and tangential interlaminar stresses exerted between the sublaminates at the delamination front were deduced, so that the mode-mixity angle could be obtained explicitly and a mixed-mode growth criterion could be applied. Recently, the above model has been extended to include delamination growth under cyclic compression [26]. The present paper considers a superficial layer as a thin film partly bonded to an infinite substrate by means of an elastic interface made of normal and tangential springs. The above delaminated plate model is here suitably modified to consider a film of infinite length over a substrate of infinite thickness. Accordingly, new explicit expressions are determined for the solution of the equilibrium problem, in particular for the displacements of the film and the interface stresses. Hence, the strain energy release rate is determined, together with its modal components, by means of the virtual crack closure technique. Finally, the mode-mixity angle is determined as a function of the applied stress and the size of the debonded region. The results obtained are able to predict some experimentally observed features, such as the arrest of the crack growth due to the predominance of mode II over mode I, as the load grows higher and the debonded region extends [27]. Moreover, the model confirms some recent results concerning stiff films on compliant substrates [28-29].

Formulation of the problem

We consider the plane-strain problem of a thin film of thickness H_f , bonded to a substrate of infinite extent, except for a portion of length $2a$. A rectangular coordinate system OXZ is fixed with the origin at the centre of the debonded region, the X -axis and the Z -axis parallel and normal to the external surface, respectively (Fig. 1).

Both the film and the substrate are assumed to behave as linearly elastic solids. Let E_f and ν_f be the Young modulus and the Poisson ratio of the film, respectively. Let E_s and ν_s be those of the substrate. Since we consider a plane-strain problem, it is convenient to introduce the reduced moduli, $\bar{E}_f = E_f / (1 - \nu_f^2)$ and $\bar{E}_s = E_s / (1 - \nu_s^2)$.

The bonded parts of the film are connected to the underlying substrate by means of an elastic interface, supposed without thickness and modelled as a continuous distribution of linearly elastic springs placed in both the X and Z directions, characterised by the spring constants k_x and k_z , respectively.

A compressive strain, ε_A , acting along the X -axis, is prescribed far away from the debonded region. Consequently, at infinite distance, the film and the substrate are subjected to the compressive stresses $\sigma_f^\infty = \bar{E}_f \varepsilon_A$ and $\sigma_s^\infty = \bar{E}_s \varepsilon_A$.

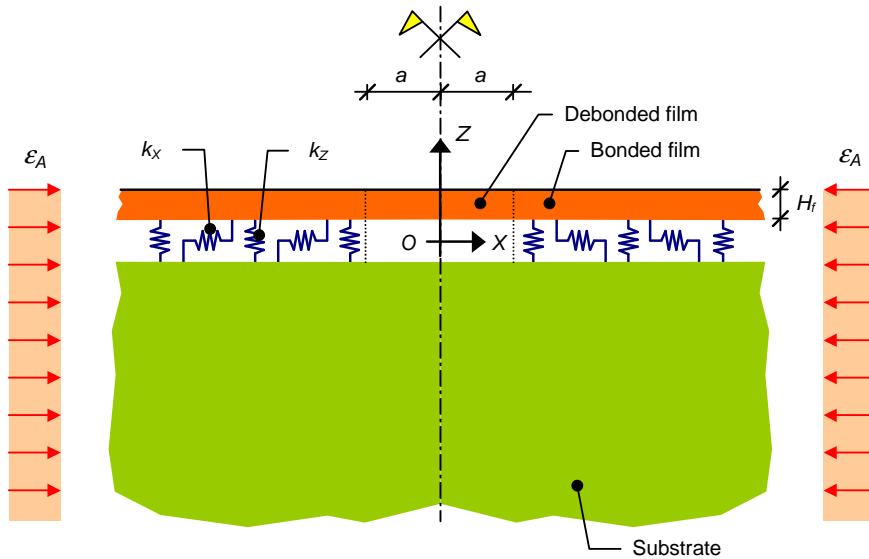


Figure 1. Thin film bonded to a substrate through an elastic interface.

We denote with u and w the displacements along the X -axis and the Z -axis, respectively. The subscripts f and s will refer to the film and to the substrate. Under the above assumptions, the differential equations of the equilibrium problem are obtained from von Kármán's plate theory for the debonded film,

$$\frac{\partial^4 w_f}{\partial X^4} + \frac{1}{\lambda^2} \frac{\partial^2 w_f}{\partial X^2} = 0 \quad \text{and} \quad \frac{\partial u_f}{\partial X} + \frac{1}{2} \left(\frac{\partial w_f}{\partial X} \right)^2 + \frac{\sigma_f}{\bar{E}_f} = 0, \quad \text{for } 0 \leq X < a, \quad (1a, b)$$

and from Kirchhoff's classical plate theory for the bonded film,

$$\frac{\partial^4 w_f}{\partial X^4} + \frac{1}{\mu^4} w_f = 0 \quad \text{and} \quad \frac{\partial^2 u_f}{\partial X^2} - \frac{1}{\omega^2} (u_f - u_s) = 0, \quad \text{for } a \leq X, \quad (2a, b)$$

and for the substrate (supposed rigid in bending),

$$\frac{\partial u_s}{\partial X} + \frac{\sigma_s}{E_s} = 0. \quad (3)$$

In the above expressions, σ_f and σ_s are the axial stresses in the debonded film and in the substrate, respectively, and the following auxiliary constants have been introduced

$$\lambda^2 = \frac{1}{12} \frac{\bar{E}_f H_f^2}{\sigma_f}, \quad \mu^4 = \frac{1}{12} \frac{\bar{E}_f H_f^3}{k_z} \quad \text{and} \quad \omega^2 = \frac{\bar{E}_f H_f}{k_x}. \quad (4a, b, c)$$

The differential problem is completed by proper boundary conditions, whose expressions are here omitted for brevity's sake.

Delamination buckling

The stated equilibrium problem can be solved explicitly [24]. Leaving out the details of the calculation, we limit ourselves to presenting here the main results.

The stress in the film at which local buckling occurs, σ_B , is obtained by solving for λ the equation

$$2\lambda\mu \cos \frac{a}{\lambda} + (2\lambda^2 - \mu^2) \sin \frac{a}{\lambda} = 0. \quad (5)$$

So, the transverse displacement of the film in the post-critical phase is

$$w_f(X) = \begin{cases} W_f \left(\cos \frac{X}{\lambda} + \frac{4\lambda^4 + \mu^4}{4\lambda^3 \mu} \sin \frac{a}{\lambda} \right), & \text{for } 0 \leq X < a, \\ W_f \frac{\mu}{4\lambda^3} \sin \frac{a}{\lambda} \left[(2\lambda^2 + \mu^2) \cos \frac{X-a}{\mu} - (2\lambda^2 - \mu^2) \sin \frac{X-a}{\mu} \right] \exp\left(-\frac{X-a}{\mu}\right), & \text{for } a \leq X, \end{cases} \quad (6)$$

where

$$W_f = 2\lambda \sqrt{\frac{a + \omega}{a - \lambda \sin \frac{a}{\lambda} \cos \frac{a}{\lambda} + 2\omega \sin^2 \frac{a}{\lambda}} \frac{\sigma_f^\infty - \sigma_B}{E_f}} \quad (7)$$

is the amplitude of the sinusoid representing the transverse displacement of the debonded film. This amplitude is zero throughout the pre-critical phase, and becomes an increasing function of the applied stress only after buckling has occurred. Further, the axial displacement of the film,

$$u_f(X) = \begin{cases} -\frac{\sigma_B}{E_f} X - \frac{W_f^2}{8\lambda} \left(\frac{2X}{\lambda} - \sin \frac{2X}{\lambda} \right), & \text{for } 0 \leq X < a, \\ -\frac{\sigma_f^\infty}{E_f} X - \left[\frac{W_f^2}{8\lambda} \left(\frac{2a}{\lambda} - \sin \frac{2a}{\lambda} \right) - a \frac{\sigma_f^\infty - \sigma_B}{E_f} \right] \exp\left(-\frac{X-a}{\omega}\right), & \text{for } a \leq X, \end{cases} \quad (8)$$

and the axial displacement of the substrate,

$$u_s(X) = -\frac{\sigma_f^\infty}{E_f} X, \quad (9)$$

are deduced. Finally, the normal and tangential interfacial stresses can be computed

$$\sigma_{zz}(X) = k_z w_f(X) \quad \text{and} \quad \tau_{zx}(X) = k_x [u_f(X) - u_s(X)]. \quad (10a, b)$$

Delamination growth

Griffith's classical criterion assumes that crack growth occurs when the energy release rate, $G = -\partial\Pi / \partial a$ (where Π is the total potential energy of the system) reaches a critical value, G_C . In its original and simplest formulation, G_C is a material constant to be determined by experiment. Nevertheless, for layered materials, experimental determinations of G_C are markedly dependent on which propagation mode (I or opening, II or sliding, III or tearing) is active in the test performed. Actually, values measured in pure mode-III tests, $G_{III C}$, are usually greater than those obtained in pure mode-II tests, $G_{II C}$, which, in turn, are much greater than the values measured in pure mode-I tests, $G_{I C}$. Under mixed-mode conditions, an intermediate value of G_C is expected, depending on which mode prevails. In these cases, in order to predict crack growth, a mixed-mode criterion must be adopted. This criterion can still be expressed by $G = G_C$, provided that G_C is considered a function of the relative amount of the different propagation modes instead of a constant. For plane problems involving the decohesion of a thin film from a substrate, the critical energy release rate can be defined as [17-18]

$$G_C(\psi) = G_{I C} \{1 + \tan^2[(1-\gamma)\psi]\}, \quad (11)$$

where the ratio $\gamma = G_{I C} / G_{II C}$ has been introduced, together with the mode-mixity angle

$$\psi = \arctan \left| \frac{\tau_{zx}(a)}{\sigma_{zz}(a)} \right|, \quad (12)$$

which measures the relative amount of mode II with respect to mode I, by ranging from 0° (pure mode-I conditions) to 90° (pure mode-II conditions).

As far as the strain energy release rate is to be determined, although it could be computed by direct calculation, it is more convenient to use Rice's integral

$$G = J = \oint_{\Gamma} \left(\phi n_x - t_x \frac{\partial u}{\partial X} - t_z \frac{\partial w}{\partial X} \right) d\Gamma, \quad (13)$$

where Γ is an arbitrary integration path around the crack front, ϕ is the strain energy density, n_x is the X-axis component of the unit normal vector of the path, t_x e t_z are the components of the stress vector. Alternatively, the strain energy release rate can be determined as

$$G = G_I + G_{II}, \quad (14)$$

where the contributions, G_I and G_{II} , relative to modes I and II can be deduced through the virtual crack closure technique. For our model, after some calculations here omitted for the sake of brevity, the modal components of G turn out to be

$$G_I = \frac{1}{8} k_z \frac{\mu^2 (2\lambda^2 + \mu^2)^2}{\lambda^4} \frac{(a+\omega) \sin^2 \frac{a}{\lambda}}{a - \lambda \sin \frac{a}{\lambda} \cos \frac{a}{\lambda} + 2\omega \sin^2 \frac{a}{\lambda}} \frac{\sigma_f^\infty - \sigma_B}{\bar{E}_f}, \quad (15a)$$

$$G_{II} = \frac{1}{2} k_x \omega^2 \left(\frac{a - \lambda \sin \frac{a}{\lambda} \cos \frac{a}{\lambda} - 2a \sin^2 \frac{a}{\lambda}}{a - \lambda \sin \frac{a}{\lambda} \cos \frac{a}{\lambda} + 2\omega \sin^2 \frac{a}{\lambda}} \right)^2 \left(\frac{\sigma_f^\infty - \sigma_B}{\bar{E}_f} \right)^2, \quad (15b)$$

and the mode-mixity angle is

$$\tan \psi = \frac{k_x}{k_z} \frac{2\lambda\omega^2}{\mu(2\lambda^2 + \mu^2)} \frac{a - \lambda \sin \frac{a}{\lambda} \cos \frac{a}{\lambda} - 2a \sin^2 \frac{a}{\lambda}}{\sin \frac{a}{\lambda} \sqrt{(a - \lambda \sin \frac{a}{\lambda} \cos \frac{a}{\lambda} + 2\omega \sin^2 \frac{a}{\lambda})(a + \omega)}} \sqrt{\frac{\sigma_f^\infty - \sigma_B}{\bar{E}_f}}. \quad (16)$$

Application

As an application, we consider the case of a thin superficial alumina layer (Al_2O_3) thermally grown on a nickel-based bond coating, such as those used for protecting superalloys against corrosion. According to literature [27], the material properties of the film are taken as $E_f = 375$ GPa and $\nu_f = 0.27$, and those of the substrate as $E_s = 188$ GPa and $\nu_s = 0.31$. The thickness of

the film is $H_f = 5 \mu\text{m}$. Moreover, we assume that the spring constants of the interface can be expressed as

$$k_x = \frac{2}{\frac{H_f}{10} \left(\frac{1}{G_f} + \frac{1}{G_s} \right)} \quad \text{and} \quad k_z = \frac{2}{\frac{H_f}{10} \left(\frac{1}{E_f} + \frac{1}{E_s} \right)}, \quad (17a, b)$$

so we obtain $k_x = 1.93 \times 10^8 \text{ N/mm}^3$ and $k_z = 5.01 \times 10^8 \text{ N/mm}^3$, respectively.

Figure 2a shows the buckling stress, σ_B , as a function of the half-length of the debonded region, a , as computed through Equation (5). Assuming that an initial debonding with size $a = a_0$ is present, the applied stress at which buckling will take place can be deduced. Conversely, for each value of the applied stress, one can determine the maximum debonding size not susceptible of buckling. For instance, $a_0 = 100 \mu\text{m}$ yields a buckling stress $\sigma_B = 804.1 \text{ MPa}$, quite lower than the stress predicted by the thin film model, $\sigma_{B,TFM} = \pi^2 \bar{E}_f (H_f/a)^2 / 12 = 831.7 \text{ MPa}$. For the same initial debonding size, Figure 2b shows the structural response in the pre- and post-critical phases, in the plane of the applied stress, σ_f^∞ , and the transverse displacement of the mid-span of the film, $w_f(0)$, according to Equations (6) and (7).

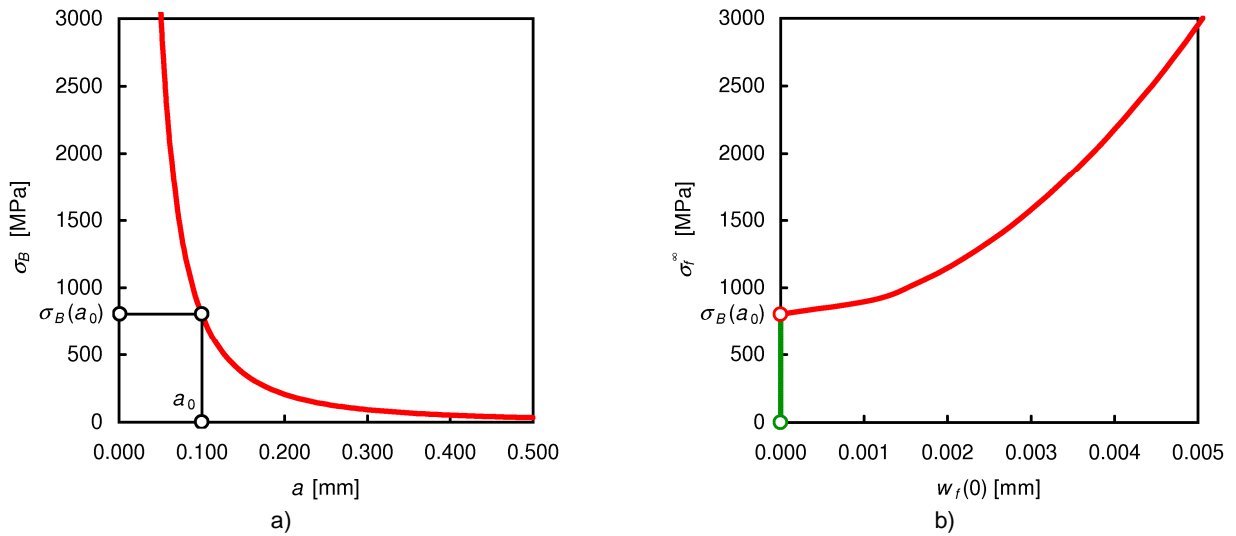


Figure 2. Delamination buckling: a) buckling stress vs. debonding size. b) applied stress vs. transverse displacement.

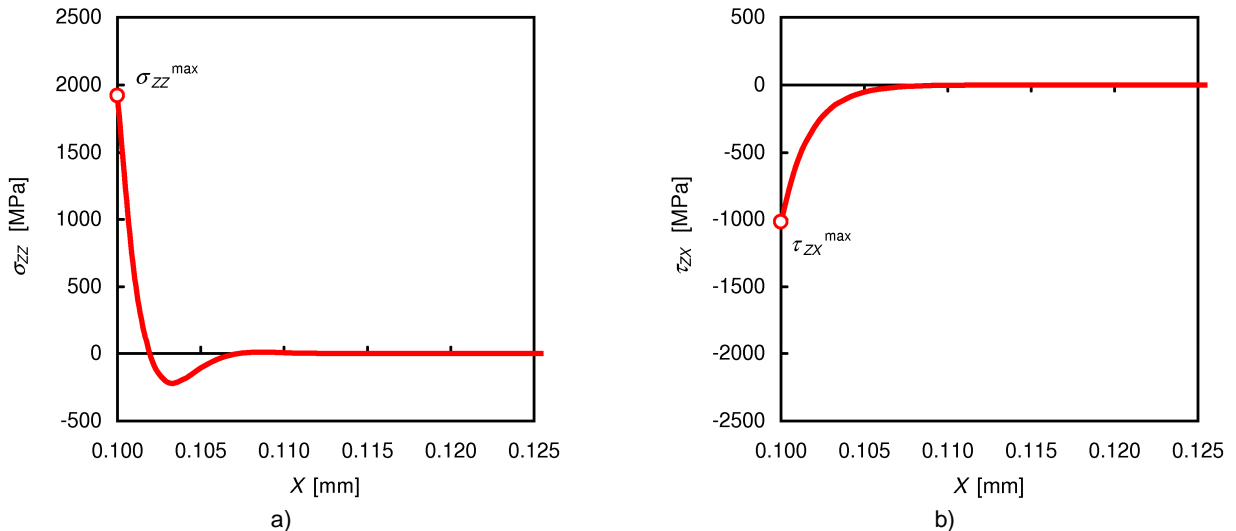


Figure 3. Interfacial stresses: a) normal stress vs. X-coordinate; b) tangential stress vs. X-coordinate.

Figures 3a and 3b show the normal and tangential interfacial stresses, σ_{zz} and τ_{zx} , respectively, arising in the bonded part of the film during the post-critical phase, as computed through Equations (8), (9) and (10). In particular, the above figures

correspond to an applied stress $\sigma_r^\infty = 1466.2$ MPa (which is equal to the stress, σ_G , defined below, corresponding to incipient crack growth). Both the components of stress attain a peak value at the crack front and then undergo rapid decay as the X-coordinate increases. Furthermore, we notice that the normal component, σ_{zz} , is positive right behind the crack front, where the substrate is consequently tensioned, and negative after a short distance, where the substrate is compressed. Successive oscillations in this stress component decay exponentially. A qualitatively similar response, although on a different order of magnitude, has been observed in recent studies concerning thin films on compliant substrates [29].

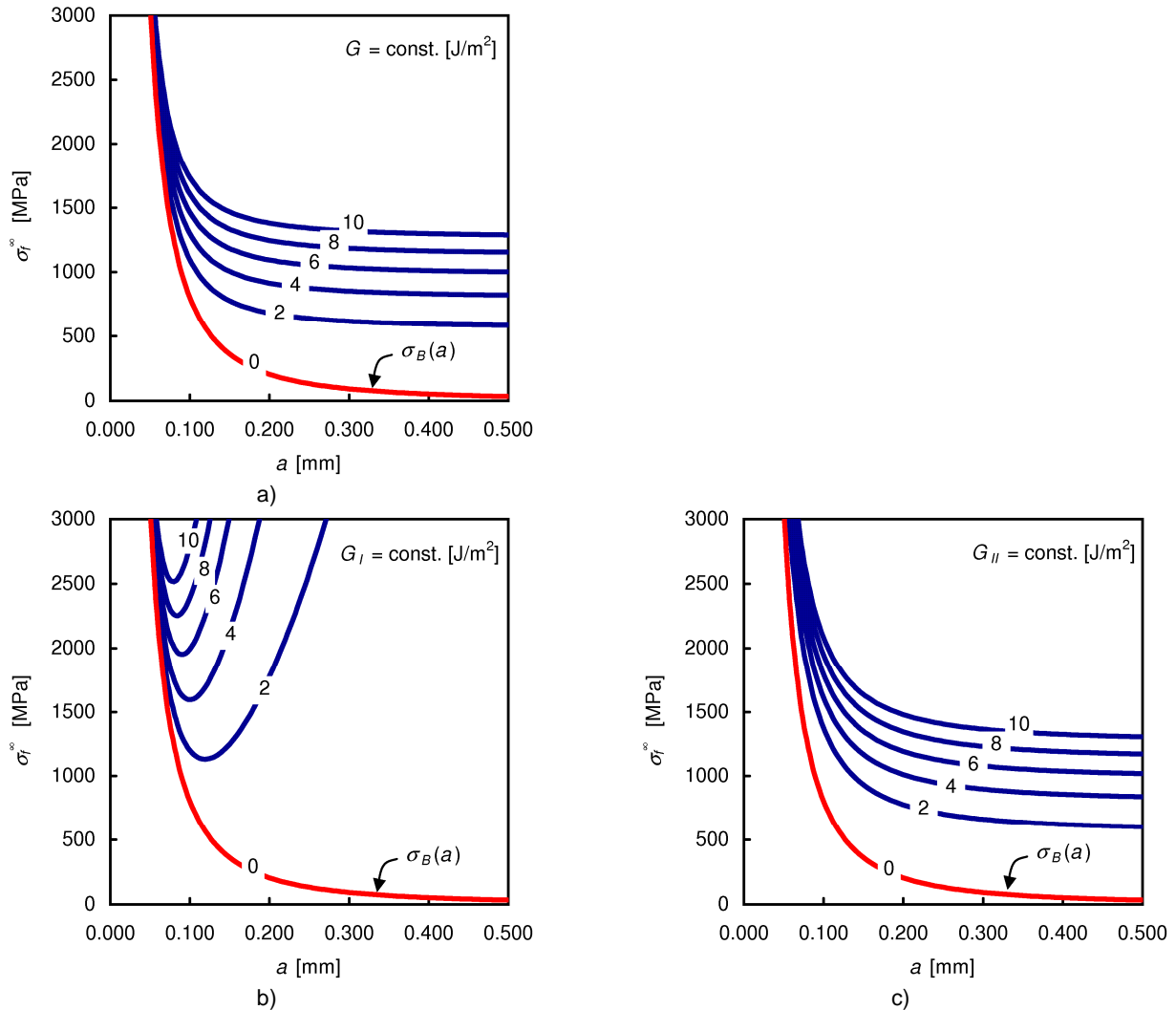


Figure 4. Strain energy release rate: a) total; b) mode-I component; c) mode-II component.

Figures 4a, 4b and 4c show, respectively, the contour plots of the strain energy release rate, G , and its modal components, G_I and G_{II} , as given by Equations (14) and (15). Along the contour lines of G (Fig. 4a), the applied stress, σ_r^∞ , is a decreasing function of a , so that Griffith's classical growth criterion ($G = G_c$) would predict unstable crack growth for any a . Along the G_I -contour lines (Fig. 4b), the applied stress, σ_r^∞ , is initially a decreasing function of a , it then reaches a minimum and afterwards becomes an increasing function. Thus, if a pure mode-I growth criterion were assumed ($G_I = G_{Ic}$), then stable growth would be predicted for debonding sizes greater than the value corresponding to that minimum. On the contrary, along the G_{II} -contour lines (Fig. 4c), the applied stress, σ_r^∞ , is a decreasing function of a , so that a pure mode-II criterion ($G_{II} = G_{IIc}$) would always predict unstable growth. To sum up, the above findings further confirm the need of a mixed-mode criterion in order to get predictions consistent with experiments, which agree with reporting stable crack growth and crack arrest [4-7, 27].

A main difficulty in modelling the process of delamination buckling and growth is that the mode-mixity is not a constant, but undergoes a characteristic evolution during the post-critical phase. The proposed model is able to predict this evolution. Figure 5a represents the contour plot of the mode-mixity angle, ψ , as given by Equation (16). This parameter is zero at incipient buckling (red curve) and then increases as either the applied stress or the length of the debonded region grows. Hence, a

transition from the opening (I) to the sliding mode (II) occurs as the process develops. Figure 5b represents the contour plot of the mixed-mode critical energy release rate, computed according to definition (11) and assuming $G_{IC} = 5.3 \text{ J/m}^2$ and $\gamma = 0.3$ [27]. We notice that upon buckling (red curve), pure mode-I conditions exist and, consequently, $G_C(\psi) = G_C(0^\circ) = G_{IC}$; instead, as ψ increases, $G_C(\psi)$ increases significantly as well (for $\psi = 90^\circ$; it would be equal to $G_{IIc} = 25.7 \text{ J/m}^2$).

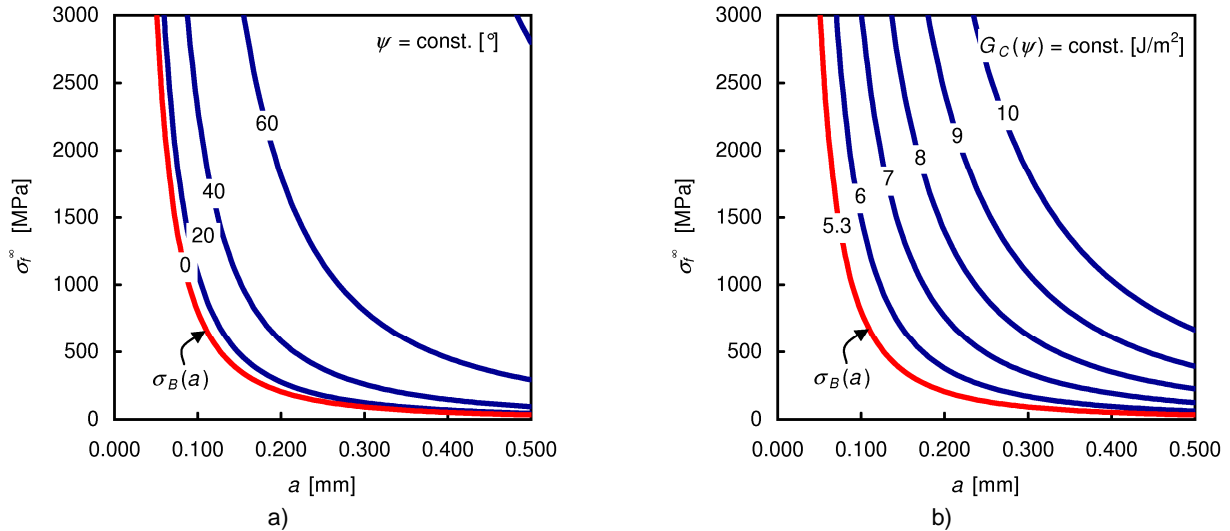


Figure 5. Mixed-mode growth criterion: a) mode-mixity angle; b) critical energy release rate.

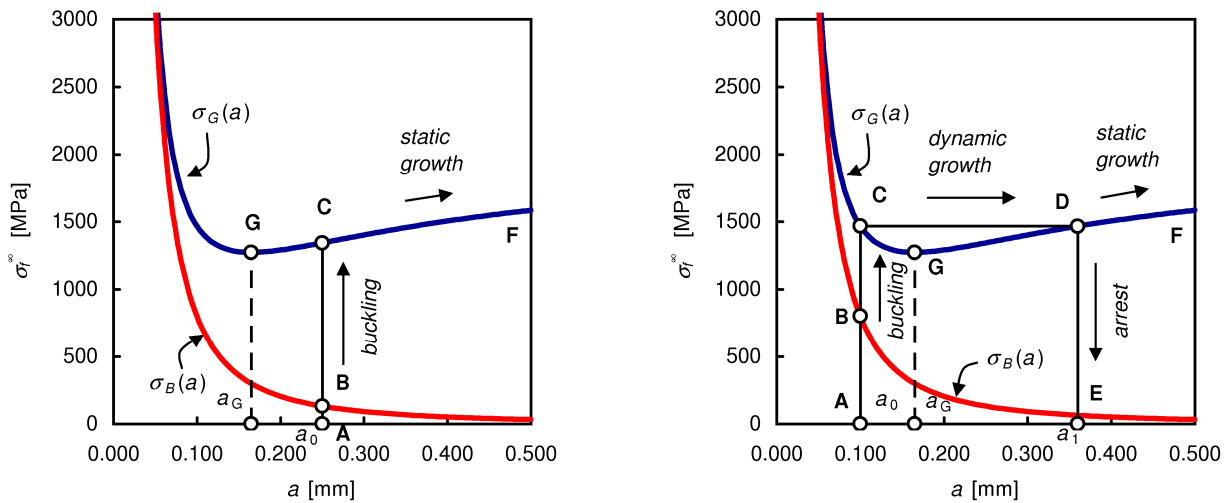


Figure 6. Buckling stress and growth stress: a) buckling-driven decohesion for $a_0 > a_G$; b) case $a_0 < a_G$.

The applied stress at which crack growth occurs, σ_G , can be predicted by solving for σ_c^* the equation $G = G_C(\psi)$. Thus, by putting together Equations (11), (14), (15) and (16), the growth stress can be obtained. This is shown in Figures 6a and 6b (blue curve) as a function of a , together with the buckling stress (red curve), σ_B . The growth stress exhibits a minimum for $a = a_G$ (point **G**), whose mechanical meaning can be highlighted by following the possible load histories on the above graphs. Let us suppose that an initial debonding of size $a_0 > a_G$ is present (Fig. 6a). Upon loading, the point representing the status of the system moves from point **A** to **B** (pre-critical phase). At **B**, the film buckles and, if the applied stress is further increased, it enters the post-critical phase. During this (from point **B** to **C**), the strain energy release rate increases until it equals the critical value at point **C**. Afterwards, crack growth occurs with both the stress and the debonding size increasing along the curve **CF**. A different behaviour is predicted if the initial debonding has size $a_0 < a_G$ (Fig. 6b). The pre- and post-critical phases (from point **A** to **C**) are similar to the previous case. But, when the point representing the status of the system reaches **C**, the applied stress cannot be further increased, in a quasi-static fashion, because of the descent of the growth curve towards point **G**. Actually, a dynamic crack growth is expected to take the system from point **C** to **D**. Here, if the applied stress is increased, then static growth takes place along the curve **CF**. Otherwise, the crack will arrest at a size corresponding to a_1 .

Conclusions

In the foregoing we have set forth a mechanical model for the mixed-mode buckling-driven decohesion of a thin superficial layer from an underlying substrate loaded in compression. Despite its apparent simplicity, which allowed us to deduce an explicit solution, the model is able to predict some experimentally observed features, such as the arrest of the decohesion growth due to the predominance of mode II over mode I, as the load grows higher and the size of the debonded region extends. Moreover, the model appears a good candidate for describing some phenomena characterising the behaviour of thin films on compliant substrates. Further work is planned to validate the model through comparison of the theoretical predictions with experimental results and to extend the plane-strain model to more realistic geometries of circular and elliptic debondings.

References

1. Garg, A.C., "Delamination – A damage mode in composite structures", *Eng. Fract. Mech.*, **29**, 557-584 (1988).
2. Bolotin, V.V., "Delaminations in composite structures: its origin, buckling, growth and stability", *Compos. Part B-Eng.*, **27**, 129-145 (1996).
3. Cheng, S.-H., Lin, C.-C. and Wang, J.T.-S., "Local buckling of delaminated sandwich beams using continuous analysis", *Int. J. Solids Struct.*, **34**, 275-288 (1997).
4. Evans, A.G. and Hutchinson, J.W., "On the mechanics of delamination and spalling in compressed films", *Int. J. Solids Struct.*, **20**, 455-466 (1984).
5. Thouless, M.D., "Combined cracking and buckling of films", *J. Am. Ceram. Soc.*, **76**, 2936-2938 (1993).
6. Christensen, R.J., Lipkin, D.M. and Clarke, D.R., "The stress and spalling behavior of the oxide scale formed on polycrystalline Ni₃Al", *Acta Mater.*, **44**, 3813-3821 (1996).
7. Gioia, G. and Ortiz, M., "Delamination of compressed thin films", *Adv. Appl. Mech.*, **33**, 119-192 (1997).
8. Kachanov, L.M., *Delamination buckling of composite materials*, Kluwer Academic Publishers (1988).
9. Chai, H., Babcock, C.D. and Knauss, W.G., "One dimensional modelling of failure in laminated plates by delamination buckling", *Int. J. Solids Struct.*, **17**, 1069-1083 (1981).
10. Madenci, E., "Delamination growth and buckling in an orthotropic strip", *Int. J. Sol. Struct.*, **27**, 1773-1788 (1991).
11. Storåkers, B. and Andersson, B., "Nonlinear plate theory applied to delamination in composites", *J. Mech. Phys. Solids*, **36**, 689-718 (1988).
12. Qu, J. and Bassani, J.L., "Interfacial fracture mechanics for anisotropic bimaterials", *J. Appl. Mech.-T. ASME*, **60**, 422-431 (1993).
13. Chow, W.T. and Atluri, S.N., "Stress intensity factors as the fracture parameters for delamination crack growth in composite laminates", *Comput. Mech.*, **21**, 1-10 (1998).
14. Yin, W.-L. and Wang, J.T.-S., "The energy-release rate in the growth of a one-dimensional delamination", *J. Appl. Mech.-T. ASME*, **51**, 939-941 (1984).
15. Sheinman, I. and Kardomateas, G.A., "Energy release rate and stress intensity factors for delaminated composite laminates", *Int. J. Solids Struct.*, **34**, 451-459 (1997).
16. Whitcomb, J. D., "Finite element analysis of instability related delamination growth", *J. Compos. Mater.*, **15**, 403-426 (1981).
17. Hutchinson, J.W., "Mixed mode fracture mechanics of interfaces", In *Metal-ceramic interfaces*, edited by Rühle, M., Evans, A.G., Ashby, M.F. and Hirth, J.P., Pergamon Press, New York, 1990, 295-306.
18. Hutchinson, J.W. and Suo, Z., "Mixed mode cracking in layered materials", *Adv. Appl. Mech.*, **29**, 63-191 (1992).
19. Audoly, B., "Mode-dependent toughness and the delamination of compressed thin films", *J. Mech. Phys. Solids*, **48**, 2315-2332 (2000).
20. Allix, O. and Ladevèze, P., "Interlaminar interface modelling for the prediction of delamination", *Compos. Struct.*, **22**, 235-242 (1992).
21. Corigliano, A., "Formulation, identification and use of interface models in the numerical analysis of composite delamination", *Int. J. Solids Struct.*, **30**, 2779-2811 (1993).
22. Point, N. and Sacco, E., "A delamination model for laminated composites", *Int. J. Solids Struct.*, **33**, 483-509 (1996).
23. Fraternali, F., "Energy release rates for delamination of composite beams", *Theor. Appl. Fract. Mech.*, **25**, 225-232 (1996).
24. Valvo, P.S., *Fenomeni di instabilità e di crescita della delaminazione nei laminati compositi*, Doctoral dissertation, University of Florence, Italy (2000).
25. Bennati, S. and Valvo, P.S., "An elastic interface model for delamination buckling in laminated plates", *Key Eng. Mater.*, **221-222**, 293-306 (2002).
26. Bennati, S. and Valvo, P.S., "Delamination growth in composite plates under compressive fatigue loads", *Compos. Sci. Technol.*, **66**, 248-254 (2005).
27. Wang, J.-S. and Evans, E.G., "Measurement and analysis of buckling and buckle propagation in compressed oxide layers on superalloy substrates", *Acta Mater.*, **46**, 4993-5005 (1998).
28. Chen, Z., Cotterell, B. and Wang, W., "The fracture of brittle thin films on compliant substrates in flexible displays", *Eng. Fract. Mech.*, **69**, 597-603 (2002).
29. Parry, G., Colin, J., Coupeau, C., Foucher, F., Cimetière, A. and Grilhé, J., "Effect of substrate compliance on the global unilateral post-buckling of coatings: AFM observations and finite element calculations", *Acta Mater.*, **53**, 441-447 (2005).